Proceedings World Geothermal Congress 2015
Melbourne, Australia, 19-25 April 2015

Geothermal Systems of Indonesia - Influence of Different Factors on the Corrosion Performance of Carbon Steel API Q125

Amela Keserovic[a,b], Ralph Bäßler[b]

[a] German Research Centre for Geosciences (GFZ), Telegrafenberg, 14473 Potsdam, Germany,

[b] Federal Institute for Materials Research and Testing (BAM), Unter den Eichen 87, 12205 Berlin, Germany

amela.keserovic@hotmail.com

Keywords: corrosion, carbon steel, electrochemistry, exposure, Sibayak, Lahendong

ABSTRACT

Among all of the existing electric power generation facilities, corrosion is considered to be the most severe on geothermal power plants. The focus of this research was set to evaluate the suitability of carbon steel API Q125 as a construction material on the geothermal sites Sibayak and Lahendong, Indonesia. The investigations were performed in the artificial geothermal brines under stagnant conditions by means of short-term electrochemical methods (Tafel extrapolation) and long-term exposure tests (up to 6 months). Furthermore, the influence of different parameters on the steels performance (temperature 70 °C, 100 °C and 175 °C, salinity 20 mg/L and 1,500 mg/L chlorides, pH 2 and 4) was assessed as well to ensure a "safer operating window" of a power plant.

The results showed carbon steel API Q125 could be suitable for application in stagnant geothermal brines up to temperatures of 175 °C and a chloride concentration of 1,500 mg/L. Its applicability is limited in highly acidic environments (pH 2).

1. INTRODUCTION

The growth in a global demand for energy, as well as the awareness of a significant climate change, have evolved a very strong incentive for utilization and expansion of clean and renewable energy resources usage.[1-3] Geothermal energy is considered as one of a few alternatives ideal for replacing conventional sources due to its consistency and reliability, and is receiving ever more attention.2,4 However, geothermal sources are found to be the most aggressive natural environments in terms of corrosion. High temperature and pressure conditions, as well as the existence of almost an entire periodic system of elements in the form of corrosive salts, represent a major threat to the integrity of the construction material, i.e. geothermal power plants.[5] Therefore, in order to achieve a safer and continuous energy production, and increase the competitiveness of geothermal energy on the world scene, a comprehensive assessment of the materials suitability is of high importance for operators and vendors. In this way, the life span of a power plant could be lengthened, while at the same time maintenance costs minimized.

Geothermal power plants consist of various construction units required for the power plant operation (separators, heat exchangers, pipelines, etc.). In order to exploit the geothermal fluid from the reservoir and transfer it to the turbine in the geothermal power plant, several hundred meters of transmission pipeline is installed, along with different equipment, necessary for plants' performance. The most commonly used materials for construction of these units are metallic materials and primarily steels, due to their excellent corrosion resistance in aggressive geothermal environments, appropriate mechanical properties and lower costs compared to other materials.[6-8]

Accounting for approximately 85% of the global annual steel production, carbon steel is the most widely used piping material.7 Despite its relatively limited corrosion resistance in aqueous solutions, especially in acidic media,[9,10] carbon steel is used in marine applications, chemical processing, petroleum production and refining, construction and metal processing equipment.[11,12] Its use is justified if the pipes and tubes replacement, due to the high corrosion rate that often occur,[13,14] is physically feasible and cost effective. Nevertheless, carbon steel has the possibility to form a compact and stable iron oxide/hydroxide layer, which acts as a physical barrier between the steel and the corrosive environment, thus reducing the corrosion rate.[15,16]

This paper presents a part of the research project that deals with investigating the suitability of different steel grades for exploitation of geothermal resources in volcanic environments.[17,18] The focus was set on assessing the suitability of carbon steel API Q125 for construction of a binary power plant on one of the two Indonesian geothermal "hotspots" – geothermal sites Sibayak (North Sumatra) and Lahendong (North Sulawesi). Considering the fact that the geothermal systems are prone to periodic changes of physicochemical parameters,[19,20] an influence of various factors on the steel performance was evaluated. The main factors that determine the corrosion rate of metals in geothermal fluids are temperature, acidity and chloride ion concentration, among the others.[21,22] The influence of these parameters on the corrosion performance of the construction material needs to be elucidated thoroughly prior to the initial design phase to ensure a "safer operating window" of a power plant.

Temperature increase was found to increase the corrosion rate of carbon steel only when the metal dissolution was controlled by the chemical reaction.[23,24] In case the corrosion was influenced by other factors, such as solubility of corrosive gases (O_2, H_2S, CO_2), formation of stable and compact corrosion product film on the steel surface, etc., the corrosion rate of carbon steel in aqueous media decreased with temperature.[25,26] High solution salinity is known to decrease the solubility of oxygen.[27] Considering the oxygen as the main species reducing on the cathode in neutral and alkaline solutions, the metal dissolution rate decreases with the salt content increase.[28] However, an increase in chloride and sulphate concentration could initiate localized corrosion; the aggressive ions agglomerate and chemisorb on the active sites, penetrate through the corrosion layer toward the steel surface and cause the formation of local pits which propagate to the metal matrix. Such scenario could result in a sudden pipeline breakdown

and the failure of the whole system.[15,29] It was revealed that the solution acidity has the most profound effect on the metal dissolution when pH decreases below 4.[30,31] In such environments hydrogen reduction is a dominant cathodic reaction. An increase in its rate, due to the hydrogen ion abundance, results in an increased anodic (metal dissolution) reaction rate.[15] Furthermore, hydrogen may incorporate into the corrosion product film formed on the metal surface,[32] thereby forming positively charged localized sites and promoting the adsorption of negative chloride and sulphate ions on the metal surface.[33,34]

2. EXPERIMENTAL SECTION

Influence of various parameters (T, pH, salt concentration) on the corrosion performance of carbon steel API Q125 was evaluated by means of electrochemical techniques (Tafel extrapolation) and long-term exposure tests (up to 6 months). The experiments were conducted in stagnant artificial geothermal solutions, based on the geothermal brine analysis performed on two geothermal "hotspot" sites in Indonesia – Sibayak (SBY) and Lahendong (LHD). The corresponding chemical composition of the steel and the solutions are presented in **Table 1** and **Table 2**, respectively.

Table 1: Chemical composition of carbon steel API Q125 in wt%

C	Si	Mn	P	S	Cr	Mo	Fe
0.212	0.249	1.332	0.008	0.007	0.497	0.013	bal.

The experiments were conducted at 70 °C (100 kPa), 100 °C (100 kPa) and 175 °C (900 kPa) in the artificial SBY solution to evaluate the temperature influence, whilst salt concentration and pH effects were investigated at 175 °C (900 kPa) considering the difference in the chemical composition of SBY/LHD-05 and SBY/LHD-23 brines, respectively.

Table 2: Chemical composition in mg/L and the resulting acidity of the investigated artificial geothermal solutions

	Cl^-	SO_4^{2-}	HCO_3^-	Ca^{2+}	K^+	Na^+	pH
SBY	1,500	20	15	200	250	600	4
LHD-05	21	20	15	-	6	20	4
LHD-23	1,500	1,600	-	-	200	1,000	2

At lower temperatures experiments were performed in glass vessels using water condensers. At 175 °C autoclaves made of 316L stainless steel equipped with a manometer were used. The temperature was maintained constant during tests by means of heating devices, and controlled continuously using an external temperature regulator (precision of ±3 K) with a Pt-100 sensor. Additionally, autoclaves were housed by an aluminum cylinder to avoid heat dissipation.

Due to the possibility of oxygen intrusion into the geothermal system, in the present study no method was used to remove the dissolved oxygen from the solutions. However, it must be recognized that the dissolved oxygen will be very low at 100 °C and will also be consumed by the corrosion reactions. Reducing conditions can be assumed for the long-term experiments and to some extent for the short-term experiments as well.

For each test condition and method three specimens of the investigated material were used to assure the results reproducibility. Prior to the start of experiments, the material specimens were wet-ground with 320 SiC sand paper, thoroughly rinsed with deionized water, and cleaned ultrasonically in ethanol to remove the residual impurities and dried with acetone.

2.1. Electrochemical methods

Electrochemical measurements were carried out in a standard three electrode cell, consisting of a saturated Ag/AgCl reference electrode, a Ti/TiO_2 net counter electrode and a working electrode made of the investigated carbon steel API Q125 (20 x 15 x 3 mm³) spot-welded on a nickel holder.

The measurements were performed using Gamry Potentiostatic System Model Reference 600. All of the recorded electrode potentials, mentioned in the current work, are referred to a standard Ag/AgCl reference electrode potential.

In the current study the system stabilized after several hours of immersion ($\Delta E \leq 5$ mV/10 min). In order to obtain a comparable corrosion behavior, the electrochemical methods were conducted after 24 h of immersion. Tafel extrapolation method was carried out ±200 mV vs. free corrosion potential (E_{corr}), using 0.2 mV/s sweep rate. The corrosion rate was calculated from the corrosion current density (j_{corr}), obtained from the intersection of the E_{corr} line and the Tafel branch that showed the linearity over at least one decade of j_{corr}, according to the equation:[35]

$$CR = \frac{j_{corr} \cdot EW}{F \cdot \rho} \cdot 3.15 \cdot 10^5 \quad (1)$$

where CR [mm/y] is the corrosion rate, j_{corr} [mA/cm²] is the corrosion current density, EW [g/mol] is the material equivalent mass, F (96,500 C/mol) is Faraday constant and ρ [g/cm³] is the material density.

2.2 Exposure Tests

The coupons (50 x 20 x 3 mm³) were prepared according to the ASTM G1 standard,[36] weighed on an analytical laboratory scale (precision 10^{-4} g) and completely vertically immersed in the solutions. After exposure, the corrosion products were removed

mechanically using a paper towel and a nonmetallic bristle brush, followed by chemical cleaning in an ultrasonic bath; coupons were immersed in an aqueous solution of 250 mL/L HCl (conc.) containing 3.5 g hexamethylenetetramine.[36] The coupons were subsequently weighed on the same analytical scale as prior to the exposure. The corrosion rate was determined according to the equation:[36]

$$CR = \frac{m_2 - m_1}{A \cdot t \cdot \rho} \cdot 10^3 \quad (2)$$

where CR [mm/y] is the corrosion rate, m_1 and m_2 [g] are the coupon masses before and after the exposure and removal of corrosion products, A [mm²] is the surface area of the exposed coupon, t [y] is the time of exposure and ρ [g/cm³] is the material density.

3. RESULTS AND DISCUSSION

3.1. Effect of the temperature on the corrosion behavior

In the following section temperature influence on the corrosion performance of carbon steel API Q125 in the artificial SBY geothermal solution is shown and discussed.

3.1.1. Tafel extrapolation

Typical anodic and cathodic polarization curves obtained for Q125 steel in the investigated conditions are shown in **Figure 1**. The corresponding electrochemical data are presented in **Table 3**. Ennoblement of the E_{corr} was perceived as the temperature increased, indicating the formation of a protective film at the metal/solution interface. Relatively high cathodic slopes (B_c) suggest the presence of a concentration effect,[37] caused presumably due to the accumulation of corrosion products on the electrode surface, hindering the progress of oxidizing species from the bulk solution to the reaction interface. Considering the conditions in which the curves were generated (pH 4, aerated conditions), the main cathodic reaction was oxygen reduction:

$$O_2 + 2H_20 + 4e^- \leftrightarrow 4OH^- \quad (3)$$

Similar magnitudes of anodic Tafel slopes (B_a) point out to the similar contribution of anodic reactions to the overall corrosion process and active electrode dissolution. The absence of passivity region was clearly observed, which was understandable considering the low amount of alloying elements, particularly chromium, in the metal composition (**Table 1**). Consequently, the anodic reaction was iron dissolution to ferrous ions:

$$Fe \rightarrow Fe^{2+} + 2e^- \quad (4)$$

followed by the further oxidation to ferric ions in case of sufficient oxygen supply:

$$Fe^{2+} \rightarrow Fe^{3+} + e^- \quad (5)$$

Calculated corrosion rates at different temperatures suggest a slight increase in the electrode dissolution at 100 °C. However, with further temperature increase to 175 °C the corrosion rate was reduced to values even lower than at 70 °C. Such observation could be linked to the oxygen concentration and physical properties of the system. At 100 °C, only traces of oxygen are present in the system due to its reduced solubility. In such conditions iron oxidation is not complete and only ferrous compounds are formed, resulting in the formation of unstable and loose corrosion product film on the electrode surface, enabling the contact of the electrode surface with the corrosive environment. However, upon increasing the temperature of the closed system to 175 °C, the system pressure increased as well, leading to the increase of the oxygen partial pressure and its solubility in the solution. Such behavior results in the formation of stable adherent corrosion product film, consisting of presumably ferric oxides (mainly magnetite) due to the disproportionation and recrystallization of initially formed Fe – hydroxide layer.

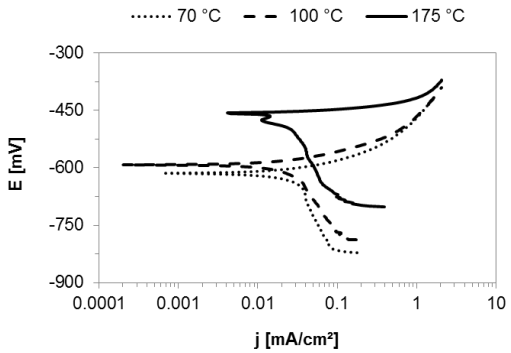

Figure 1: Potentiodynamic polarization curves of Q125 steel in the artificial SBY geothermal brine at different temperatures

3.1.2. Exposure tests

Calculated corrosion rates after exposure of Q125 steel in the SBY solution at different temperatures are depicted in **Figure 2**. Reduction in the corrosion rates of the immersed coupons is shown, suggesting the formation of a stable and adherent corrosion

film on the metal surface with time. However, after 3 months of exposure at 100 °C the rate slightly increased, which could be attributed to the corrosion products falling off due to the vertical position of the coupons in the tested vessels. Nevertheless, the corrosion rate was continuously highest at 100 °C, whilst at 175 °C lowest, thus corroborating the results obtained with Tafel extrapolation method. The discrepancy in the magnitude of the rates calculated with Tafel and the weight loss method could be linked to the fact that Tafel extrapolation method, performed after only 24 h of immersion, did not take into consideration the corrosion products formation on the metal surface in comparison to the long-term exposure tests.

Table 3: Electrochemical data of Q125 steel obtained by Tafel extrapolation method in the artificial SBY geothermal brine at different temperatures

T [°C]	B_a [mV/dec]	B_c [mV/dec]	j_{corr} [mA/cm²]	E_{corr} [mV]	CR [mm/y]
70	55	399	0.0254	-614	0.29
100	62	317	0.0273	-593	0.32
175	38	201	0.0225	-553	0.26

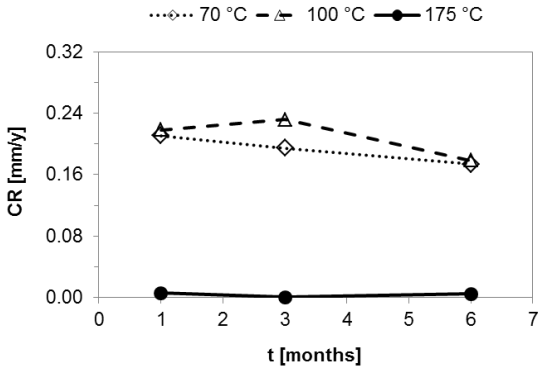

Figure 2: Corrosion rate of Q125 steel during long-term exposure tests in the artificial SBY geothermal brine at different temperatures

Cross section surface analysis of the exposed coupons shown in **Figure 3** revealed the formation of a much thicker corrosion film at 100 °C (32 µm – 58 µm) compared to the one formed at 175 °C (4 µm – 24 µm). Considering the lower metal dissolution rate at the latter temperature, the corrosion product layer was obviously more stable, adherent and compact, impairing the oxygen diffusion toward the metal surface, thus reducing the corrosion rate. On the other hand, the layer formed at 100 °C was possibly porous due to the lower oxygen content that hindered the formation of a stable and compact ferric oxide layer. In this way, the diffusion of corrosive species toward the metal surface was enabled.

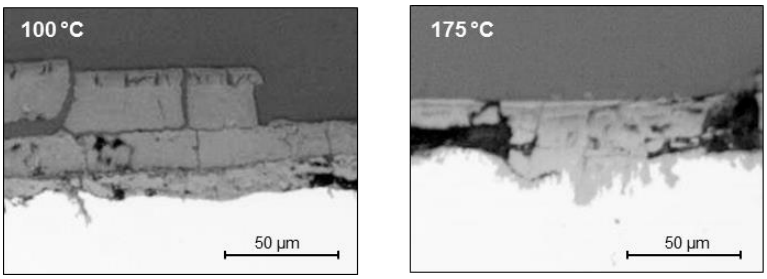

Figure 3: Cross sections of Q125 steel coupons exposed for 6 months in the artificial SBY geothermal brine at different temperatures

3.2. Effect of concentration on the corrosion behavior

In this section, influence of the chloride concentration on the corrosion performance of carbon steel API Q125 is discussed. The metal specimens were exposed to artificial geothermal brines at 175 °C containing 20 mg/L (LHD-05) and 1,500 mg/L (SBY) chlorides, respectively.

3.2.1. Tafel extrapolation

Typical anodic and cathodic polarization curves obtained for Q125 steel in the investigated conditions are shown in **Figure 4**. The corresponding electrochemical data are presented in **Table 4**. Corrosion potential shifted to more negative (cathodic) potentials with the addition of salts to the solution. This could be attributed to the oxygen content, which is lower in the more concentrated

solution (SBY) due to the "salting out" phenomenon;[38] the presence of more ionic species in the SBY solution reduces the affinity of the non-polar oxygen molecules to the polar water, resulting in decreased oxygen solubility in the solution. Considering that only in the presence of sufficient oxygen concentration stable and adherent ferric oxides could form on the surface, in the solution containing higher salt concentration mostly soluble corrosion products form.[39] Therefore, the surface tended to be more active than in the solution containing lower amount of salt. Furthermore, chlorides (the main ionic species in the SBY solution) form soluble, unstable complexes with iron, hygroscopic in nature, and in this way enhance the surface electrolyte formation. As a consequence, corrosion attack was further stimulated and the metal surface exhibited more active potentials. However, according to the corrosion rates calculations (**Table 4**), the electrode dissolution rates were higher in the less concentrated solution (LHD-05). Again, this was probably caused by the lower oxygen concentration. Nevertheless, in this case lower amount of oxygen resulted in a decrease of cathodic reaction rate considering the conditions in which the curves were generated (pH 4, aerated conditions) and thus, the oxygen being the main oxidizing specie (Equation (5)). Moreover, lower salt content resulted in a lower viscosity of the medium and consequently, higher diffusion rates of ionic species, based on the Stokes-Einstein equation,[40]

$$D_i = \frac{kT}{6\pi r_i \eta} \tag{8}$$

where D_i is the diffusion coefficient of ion, k is the Boltzmann constant, r_i is the effective radius of ion, η is the viscosity of solutions and T is the absolute temperature.

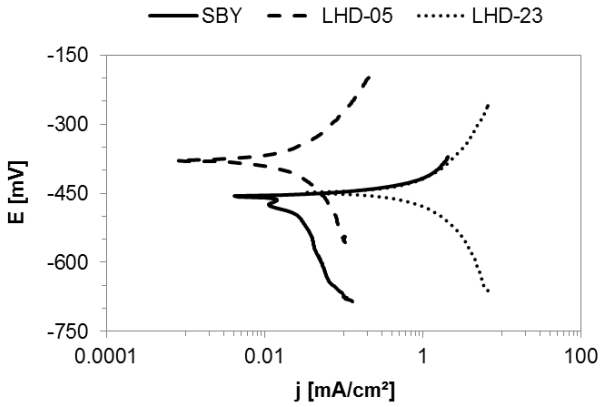

Figure 4: Potentiodynamic polarization curves of Q125 steel at 175 °C as a function of the solution concentration and acidity

Table 4: Electrochemical data of Q125 steel obtained from polarization measurements as a function of the solution concentration and acidity

	B_a [mV/dec]	B_c [mV/dec]	j_{corr} [mA/cm²]	E_{corr} [mV]	CR [mm/y]
SBY	38.0	201.3	0.0225	-502.3	0.26
LHD-05	113.3	125.5	0.0274	-375.5	0.32
LHD-23	256.7	263.9	1.3500	-462.8	15.62

3.2.2. Exposure tests

Calculated corrosion rates after exposure of Q125 steel in the SBY and LHD-05 solutions at 175 °C are depicted in **Figure 5**. Relatively low uniform corrosion rates (< 20 μm) irrespective of the salt concentration were observed. However, lower corrosion rates were recorded in the more concentrated solution (SBY). Such finding corroborates the results obtained with the Tafel extrapolation method.

3.3. Efect of pH on the corrosion behavior

Effect of pH on the corrosion performance of carbon steel API Q125 was investigated in the artificial geothermal brines pH 4 (SBY) and pH 2 (LHD-23) at 175 °C. The corresponding results and the discussion are shown in the further text below.

3.3.1. Tafel extrapolation

Typical anodic and cathodic polarization curves obtained for Q125 steel in the investigated conditions are shown in **Figure 4**. The corresponding electrochemical data are presented in **Table 4**. Similar E_{corr} values suggest similar surface activity of the electrodes irrespective of the solution acidity. However, significant shift of the polarization curves toward higher current densities was observed in the more acidic solution (LHD-23), pointing out the higher metal dissolution rates. Same contribution of the cathodic reaction to the overall corrosion reaction was indicated by the similar cathodic Tafel slopes (B_c). The main cathodic reaction in the LHD-23 brine was most certainly hydrogen reduction due to the acidic conditions in which the reaction took place:

$$2H^+ + 2e^- \rightarrow H_2 \tag{9}$$

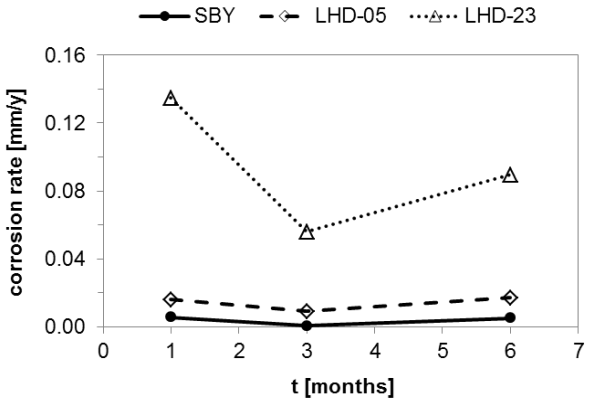

Figure 5: Corrosion rate of Q125 steel during long-term exposure tests at 175 °C as a function of the solution concentration and acidity

Similar values of the corrosion layer thickness irrespective of the solution concentration (approximately 20 μm) point out that the lower corrosion rates in the SBY solution were probably caused by the lower diffusion coefficient of ionic species, due to the higher solution viscosity, as already suggested. However, cross section analysis of the coupons revealed the formation of pits in the latter conditions. This is reasonable considering the presence of chloride ions, responsible for localized corrosion.

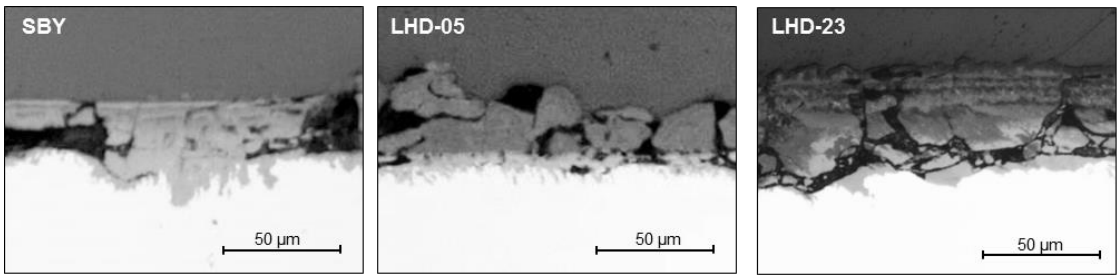

Figure 6: Cross sections of Q125 steel coupons exposed for 6 months at 175 °C in solution of different concentration and acidity

Substantially high cathodic and anodic Tafel slopes (B_c, B_a) in the latter conditions suggest that the kinetics of both cathodic and anodic reactions were controlled by the mass transfer caused by the metal cations accumulation and/or hydrogen bubbles formation on the electrode surface. pH decrease in LHD-23 solution clearly promoted metal dissolution considering the corrosion rates of one order of magnitude higher than in the less acidic conditions (SBY).

3.3.3. Exposure tests

Calculated corrosion rates after exposure of Q125 steel in the SBY and LHD-05 solutions at 175 °C are depicted in **Figure 5**. pH decrease caused a substantial increase in the corrosion rates of carbon steel API Q125 during the long-term exposure tests, pointing out the strong influence of an increased hydrogen content on the corrosion rate. Cross section analysis of the exposed coupons showed an appreciable amount of corrosion products accumulated on the surface, resulting in the layer thickness of approximately 84 μm. Considering the high corrosion rates, the layer was porous and contained a large amount of diffusion paths enabling the migration of ionic species through it. Moreover, higher local penetration rates into the metal surface were observed, which could be linked to the increased sulphate content in the LHD-23 solution.

4. CONCLUSION

Suitability of carbon steel API Q125 as a construction material for geothermal power plants on Sibayak and Lahendong geothermal fields in Indonesia was investigated by means of short-term electrochemical methods and long-term exposure tests. Considering the differences in the physicochemical composition of the geothermal brines, influence of different factors (T, salt, pH) was evaluated. The major conclusions obtained from the study are as follows:

- Increasing the temperature of the system a more stable and compact corrosion layer was formed on the steel surface exposed to the SBY solution, resulting in a corrosion rate decrease.
- Higher corrosion rates were observed in the less concentrated solution (LHD-05) due to the higher oxygen content and higher diffusion rates of ionic species.
- Corrosion layer formation was retarded in the solution pH 2 (LHD-23) resulting in the higher corrosion rates.

Accordingly, carbon steel API Q125 could be suitable for application in stagnant geothermal brines with a composition similar to SBY and LHD-05 up to 175 °C and 900 kPa due to the relatively low and within the acceptable limits corrosion rates. Its

applicability is limited in highly acidic environments such as LHD-23 (pH 2). However, additional crevice and stress corrosion susceptibility tests, as well as influence of the dynamic conditions on the steel performance, should be evaluated in order to obtain a comprehensive assessment of the alloy's applicability for the geothermal environments.

5. ACKNOWLEDGMENTS

The authors would like to acknowledge the German Federal Ministry of Education and Research for its financial support within the project Sustainability concepts for exploitation of geothermal reservoirs in Indonesia – capacity building and methodologies for site deployment under grant 03G0753A, BMBF. The support of the Pertamina Geothermal Energy team in Jakarta, as well as at Lahendong site, including the access to the data and the field is highly appreciated. The authors thank PGE for the permission to publish this paper.

REFERENCES

1. Lund, J. W., D. H. Freeston and T. L. Boyd (2011). Direct utilization of geothermal energy 2010 worldwide review. *Geothermics* 40(3) 159-180.

2. Rybach, L. (2010). Status and prospects of geothermal energy. World Geothermal Congress 2010, Bali, Indonesia.

3. Sasradipoera, D. S. and D. Hantono (2003). Strategies for developing Lahendong geothermal field, Indonesia. Twenty-Eighth Workshop on Geothermal Reservoir Engineering, Stanford University, Stanford, California.

4. Zaidi, S. H. (2010). Geothermal Energy for Sustainable Development: An Expanded Role in Indonesia's Energy Supply Chain. World Geothermal Congress 2010, Bali, Indonesia.

5. Stapleton, M. (2002). Scaling and Corrosion in Geothermal Operation. Nevada, USA, PowerChem Technology.

6. Conover, M., P. Ellis and A. Curzon (1980). Material Selection Guidelines for Geothermal Power Systems - An Overview. Geothermal Scaling and Corrosion: Symposia, New Orleans, LA, ASTM International.

7. Rafferty, K. D. (1998). Piping. Oregon, USA, Oregon Institute of Technology.

8. Toolbox, T. E. *http://www.engineeringtoolbox.com/piping-materials-cost-ratios-d_864.html* [*online*] [Accessed 25.02.2014].

9. Badr, G. E. (2009). The role of some thiosemicarbazide derivatives as corrosion inhibitors for C-steel in acidic media. *Corrosion Science* 51(11) 2529-2536.

10. Tao, Z., et al. (2012). A study of differential polarization curves and thermodynamic properties for mild steel in acidic solution with nitrophenyltriazole derivative. Ibid. 60 205-213.

11. Fouda, A. S., G. Y. Elewady and M. N. El-Haddad (2011). Corrosion inhibition of carbon steel in acidic solution using some azodyes. *Canadian J Scientific and Industrial Research* 2(1) 1-18.

12. Katariya, M. N., A. K. Jana and P. A. Parikh (2013). Corrosion inhibition effectiveness of zeolite ZSM-5 coating on mild steel against various organic acids and its antimicrobial activity. *Journal of Industrial and Engineering Chemistry* 19(1) 286-291.

13. Panossian, Z., et al. (2012). Corrosion of carbon steel pipes and tanks by concentrated sulfuric acid: A review. *Corrosion Science* 58 1-11.

14. Mueller, J., et al. (2010). Laboratory Results of Corrosion Tests for EGS Soultz Geothermal Wells. *Proc. World Geothermal Congress (Bali, 2010).*

15. Revie, R. W. (2000). *Uhlig's Corrosion Handbook*. 2nd ed: John Wiley & Sons.

16. Bartoň, K. and V. Marek (1970). Einfluß des entstehenden Rostes auf den Verlauf der atmosphärischen Korrosion von Stahl. *Materials and Corrosion* 21(3) 182-184.

17. Keserovic, A. and R. Bäßler (2013). Material Evaluation for Application in Geothermal Systems in Indonesia. *NACE Corrosion 2013*. Orlando, FL.

18. Keserovic, A. and R. Bäßler (2014). Suitability of alloyed steels in highly acidic geothermal environments. *NACE Corrosion 2014*. San Antonio (TX, USA).

19. Brehme, M. (2010). Lahendong geothermal field: fluid analysis 2010. Potsdam, Germany, GFZ.

20. Brehme, M., et al. A hydrotectonic model of a geothermal reservoir supported by hydrogeology. *Geothermics*.

21. Mundhenk, N., et al. (2013a). Metal corrosion in geothermal brine environments of the Upper Rhine graben – Laboratory and on-site studies. Ibid. 46(0) 14-21.

22. Mundhenk, N., et al. (2013b). Corrosion and scaling as interrelated phenomena in an operating geothermal power plant. *Corrosion Science* 70(0) 17-28.

23. Kairi, N. I. and J. Kassim (2013). The Effect of Temperature on the Corrosion Inhibition of Mild Steel in 1 M HCl Solution by Curcuma Longa Extract. *Int. J. Electrochem. Sci* 8 7138-7155.

24. Vuppu, A. K. and W. P. Jepson (1994). The effect of temperature in sweet corrosion of horizontal multiphase carbon steel pipelines. SPE Asia Pacific Oil and Gas Conference, Society of Petroleum Engineers.

25. Stoulil, J., et al. (2013). Influence of temperature on corrosion rate and porosity of corrosion products of carbon steel in anoxic bentonite environment. *Journal of Nuclear Materials* 443(1–3) 20-25.

26. Tskhvirashvili, D., O. Vardigoreli and P. Acolsin (1972). On corrosion of metals in geothermal power plants. *Geothermics* 1(3) 113-118.

27. Schumpe, A., I. Adler and W. D. Deckwer (1978). Solubility of oxygen in electrolyte solutions. *Biotechnology and Bioengineering* 20(1) 145-150.

28. Brondel, D., et al. (1994). Corrosion in the oil industry. *Oilfield review* 6(2) 4-18.

29. Szklarska-Smialowska, Z. (2005). *Pitting and crevice corrosion*. Houston, TX: NACE International.

30. Prasetia, A. E., A. T. N. Salazar and J. S. S. Toralde (2010). Corrosion Control in Geothermal Aerated Fluids Drilling Projects in Asia Pacific. World Geothermal Congress 2010, Bali, Indonesia.

31. Magaly, F. A., et al. (2010). The Neutralization of Acid Fluids: an Alternative of Commercial Exploitation Wells on Los Humeros Geothermal Field. World Geothermal Congress, Bali, Indonesia.

32. Thomas, J. G. N. (1961). Kinetics of electrolytic hydrogen evolution and the adsorption of hydrogen by metals. *Transactions of the Faraday Society* 57 1603-1611.

33. Yu, J. G., J. L. Luo and P. R. Norton (2002). Investigation of hydrogen induced pitting active sites. *Electrochimica Acta* 47(25) 4019-4025.

34. Ningshen, S., et al. (2006). Hydrogen effects on the passive film formation and pitting susceptibility of nitrogen containing type 316L stainless steels. *Corrosion Science* 48(5) 1106-1121.

35. International, A. (2010). Standard Practice for Calculation of Corrosion Rates and Related Information from Electrochemical Measurements. West Conshohocken, PA, ASTM International.

36. International, A. (2011). Standard practice for preparing, cleaning, and evaluating corrosion test specimens. West Conshohocken, PA, ASTM International.

37. Landolt, D. (2010). *Corrosion and surface chemistry of metals*: CRC Press.

38. Groysman, A. (2010). *Corrosion for everybody*: Springer.

39. Cornell, R. M. and U. Schwertmann (2003). *The iron oxides: structure, properties, reactions, occurrences and uses*: John Wiley & Sons.

40. Goldsack, D. E. and R. Franchetto (1977). The viscosity of concentrated electrolyte solutions. I. Concentration dependence at fixed temperature. *Canadian Journal of Chemistry* 55(6) 1062-1072.